



# Bisphenol A-Induced Cell Proliferation and Mitochondrial Oxidative Stress Are Diminished via Modulation of TRPV1 Channel in Estrogen Positive Breast Cancer Cell by Selenium Treatment

Kadriye Görkem Ulu Güzel<sup>1</sup> · Mustafa Nazıroğlu<sup>2,3</sup> · Derya Ceyhan<sup>4</sup>

Received: 3 January 2020 / Accepted: 27 January 2020 / Published online: 10 February 2020  
© Springer Science+Business Media, LLC, part of Springer Nature 2020

## Abstract

Cancer cell proliferation and apoptosis are induced by overload  $\text{Ca}^{2+}$  entry. Transient receptor potential vanilloid 1 (TRPV1) as a  $\text{Ca}^{2+}$  permeable cation channel is activated by capsaicin and reactive oxygen species (ROS), although it is blocked by capsazepine and sodium selenite (Na-Se). Bisphenol A (BPA) induces estrogenic action and further stimulates the proliferation of estrogen receptor positive MCF-7 cell through excessive production ROS and  $\text{Ca}^{2+}$  influx. However, whether or not Na-Se can influence BPA-induced oxidative stress and apoptosis through modulation of TRPV1 in breast cancer cells has not drawn much attention. The MCF-7 and MDA-MB-231 breast cancer cells were divided into four treatment groups as control, Na-Se (1  $\mu\text{M}$  for 2 h), and BPA (0.1 mM for 24 h) and BPA + Na-Se. The Na-Se reduced BPA-induced increase of cell number, mitochondria oxidative stress, and TRPV1 channel activity modulation of MCF-7 cells, which was proved by the suppression of cell viability, excessive ROS production, mitochondrial membrane depolarization, lipid peroxidation, early apoptosis (Annexin-V), late apoptosis (propidium iodide) and upregulation of reduced glutathione, glutathione peroxidase, and cell death (propidium iodide/Hoechst rate). The similar effects of Na-Se were observed in the MCF-7 cells by capsazepine treatment. However, the effects of BPA were not observed in the MDA-MB-231 breast cancer cells. In conclusion, cell proliferative and oxidant effects of BPA were increased by activation of TRPV1, but its action on the values was decreased by the Na-Se treatment. The results may be a good set of preliminary data for designing animal studies on estrogenic effect of bisphenol A and antiestrogenic of selenium.

**Keywords** Apoptosis · Bisphenol A · Breast cancer cells · Oxidative stress · Selenium · TRPV1 channel

## Introduction

Bisphenol A (BPA) as a synthetic compound contains two hydroxyphenyl groups. BPA used several live materials such as baby feeding bottles, food packaging, and medical facilities. Hence, BPA is one of popular environmental toxicant [1,

2]. Thus, its continuous exposure in the environment has raised major public health concerns in cancer development [3]. There is a chemical structure similarity between BPA and estrogen hormone [4]. Hence, several reports have suggested that BPA can interact with several hormone receptors, including estrogen receptors and androgen receptors, causing adverse health effects and leading to a variety of irregularities in the reproductive system [4–6].

Calcium ion ( $\text{Ca}^{2+}$ ) is an important second messenger for several physiological functions [7]. The  $\text{Ca}^{2+}$  has also important action in cancer pathophysiology, and an increase in the intracellular  $\text{Ca}^{2+}$  concentration through activation of calcium channels in cancer cells might attenuate key aspects of tumor progression, including proliferation and metastasis [8–10]. One of those calcium channels is the non-selective cation transient receptor potential (TRP) super family [11]. One subfamily of the TRP super subfamily is TRP vanilloid 1 (TRPV1) that was first expressed in sensory neurons [12]. The TRPV1 is activated by several stimuli such as hot chili pepper component

✉ Mustafa Nazıroğlu  
mustafanaziroglu@sdu.edu.tr

<sup>1</sup> Department of Pedodontics, Faculty of Dentistry, Adnan Menderes University, Aydın, Turkey

<sup>2</sup> Neuroscience Research Center, Suleyman Demirel University, 32260 Isparta, Turkey

<sup>3</sup> Drug Discovery and Development Research Group, BSN Health, Analysis and Innovation Ltd. Inc. Teknokent, Goller Bolgesi Teknokenti, Isparta, Turkey

<sup>4</sup> Department of Pedodontics, Faculty of Dentistry, Suleyman Demirel University, Isparta, Turkey

(capsaicin, Cap), reactive oxygen (ROS), and nitrogen species [12, 13]. The presence of the TRPV1 channel expression has also been indicated in estrogen receptor positive MCF-7 breast cancer cells [14, 15]. It has been reported that cancer cell proliferation, apoptosis, and necrosis is induced in the MCF-7 cells by increased activation of the TRPV1 [15–18]. Accumulating evidences indicated that there is a direct relationship between estrogen production and breast cancer tumor development [19]. TRPV1 was activated by estrogen [20, 21], although it was blocked in dorsal root ganglion and hippocampus of rats by treatments of estrogen receptor blockers [22]. BPA may induce breast cancer proliferation via TRPV1 channel activation-induced  $\text{Ca}^{2+}$  influx and estrogenic effects, because of the presence of the chemical structure between estrogen and BPA. The subject should be clarified in the estrogen receptor positive MCF-7 and estrogen receptor negative (MCF-7) and negative (MDA-MB-231) cells.

Selenium is an essential trace element. An inorganic form of selenium is sodium selenite (Na-Se). Because Na-Se is the most common supplemental form of selenium, it can be used for treatment of several diseases. Selenium is a co-factor of glutathione peroxidase (GSHPx) antioxidant enzyme and several ROS are scavenged by the GSHPx. In addition, several cancer metabolisms such as tumor progression, DNA repair, apoptosis, and several hormone productions are modulated in the breast cancer cells by Na-Se treatments [23–25]. Oxidant effects of BPA were reported in several human, rodent, and cell line models [1, 5]. However, the protective actions of Na-Se against BPA-induced cytotoxicity and oxidative stress were reported in the lung [26], testis [27, 28], and liver of rats [29]. Antitumor and anti-apoptotic actions of selenium through modulation TRPV1 channel in MCF-7 cells [25] and dorsal root ganglion neuron [30] were recently reported, and the similar actions might occur in BPA-induced toxicity of MCF-7 cancer cells.

There is no report of selenium on the apoptosis, mitochondrial oxidative stress, and  $\text{Ca}^{2+}$  entry through modulation of TRPV1 channel in the MCF-7 and MDA-MB-231 cells following BPA treatment. Therefore, we propose that inhibition of TRPV1 in the selenium treatment might represent the mechanisms controlling upregulation of mitochondrial oxidative stress and apoptosis, and  $\text{Ca}^{2+}$  fluorescence concentration in the BPA-treated MCF-7 breast cancer cells.

## Materials and Methods

### Cell Culture

Estrogen receptor positive breast cancer (MCF-7) cell and estrogen receptor negative breast cancer (MDA-MB-231)

cells were gift from (Dr. Gamze Güney Eskiler, Sakarya University, Sakarya, Turkey). Both cell lines were cultured in a medium consisting of 90% DMEM medium with low glucose (1 g/l) (Thermo Fischer Scientific, Istanbul, Turkey), 10% heat-inactivated fetal bovine serum (Cegrogen Biotech, Stadtallendorf, Germany), and 1% antibiotic combination (streptomycin+penicillin) (Sigma-Aldrich, Istanbul, Turkey). The cells in the medium mixture were kept in a humidified atmosphere in 5%  $\text{CO}_2$  at 37 °C. The cells were tested within 24 h after plating onto the coverslips before counting in an automatic cell counter (Casy Modell TT, Roche, Germany). The cells were seeded in 4 flasks at a density of  $1 \times 10^6$  cells per flask (Thermo Fischer). In confocal microscope analyses, the cells were seeded in 35-mm glass bottom dishes (Mattek Corporation Inc., Ashland, MA, USA).

### Groups

The MCF-7 and MDA-MB-231 cells were used in the investigation of the effects of BPA in the current study. The cells were mainly divided into four groups as control, Na-Se, BPA, and BPA + Na-Se. The cells in the control group were kept in a flask containing the same cell culture medium and conditions for 26 h. Non-toxic doses of Na-Se were reported between 200 and 2 mM in literature [23, 25], although BPA was used as 0.1 mM in the MCF-7 and MDA-MB-231 cells [31]. Hence, cells in the Na-Se group were kept 24 h in the same culture condition without treatment, and then they were pre-incubated with Na-Se (1  $\mu\text{M}$ ) for 2 h as described in a previous study [25]. Cells in the BPA group were incubated with BPA (0.1 mM) for 24 h [31]. The cells in the combination group were incubated with BPA (0.1 mM) for 24 h and then incubated with Na-Se (1  $\mu\text{M}$ ) for a further period of 2 h.

### Assay of Cell Viability and Cell Number

For proliferation assay, the MCF-7 and MDA-MB-231 cells were counted by using the automatic cell counter (Casy Modell TT) as described in a previous study [32]. Briefly, the DMEM medium of the cells was removed at the end of the incubation periods for BPA and Na-Se. After diluting the cells with Casy tone solution, the cells were automatically counted in solution by the automatic cell counter. In addition to cell number, cell debris (membranes and residues of death cell) and cell viability were monitored through electrical current exclusion by the cell counter. Debris count and cell viability were expressed as  $10^6/\text{ml}$  and %, respectively.

### Determination of Live (Hoechst)/ Death (PI) Cell Rate

Live cells were investigated in a laser confocal microscope (LSM 800, Zeiss, Ankara, Turkey) fitted with a  $\times 20$  objective

by using Hoechst-33342 staining, although death cells in the microscope (LSM 800) were investigated by propidium iodide (PI) staining as described in a previous study [33]. In brief, the cells were seeded in the 35-mm glass bottom dishes and they were incubated in the culture medium and conditions were further incubated for 30 min with PI (5 µg/ml) and Hoechst 33342 (1 µM) (Cell Signaling Technology). Images were recorded by using a ZEN program. Rate of live and death cell was expressed as %.

### Apoptosis (Annexin V and PI) Assay by Laser Confocal Microscope

Annexin V-FITC is an early apoptotic dye and it connects to the membranes of apoptotic cells, displaying a green characteristic staining pattern. PI is a membrane impermeable dead cell stain instead of apoptosis. The state of the cell determines the ability of PI staining to distinguish between viable and apoptotic cells and it has been used indicator of late apoptosis [34]. The protective effects of Na-Se against BPA-induced early and late apoptosis were measured in the laser confocal microscope (LSM-800) fitted with a × 20 objective by using the commercial Annexin V-FITC (1 µl for 15 min incubation) and PI (10 µl for 15 min incubation) apoptosis dyes at room temperature in dark (Santa Cruz Biotechnology Inc. Istanbul, Turkey) as described in a previous study [32]. Fluorescence intensity of each cell as arbitrary unit was measured by using ZEN program and analyzed using Image J/Imaris software. The results of Annexin V-FITC and PI were expressed as the mean fluorescence intensity as arbitrary unit/cell.

### Detection of Intracellular Ca<sup>2+</sup> Fluorescence Intensity Concentration Through TRPV1 Activation

Intracellular changes in the Ca<sup>2+</sup> fluorescence concentration in the MCF-7 cell lines were analyzed in the glass bottom dishes by using Fluo-3 fluorescent dye (Calbiochem, Darmstadt, Germany). Fluorescence intensity of Fluo-3 was excited by a 488-nm argon laser from the confocal microscope (LSM 800), because Fluo-3 is a single wavelength excitation and emission dye [30, 32, 33]. In some experiment of BPA group, the cells were treated with

TRPV1 antagonist (Cpz and 100 µM) to inhibit Ca<sup>2+</sup> entry before stimulation of TRPV1 (Cap and 10 µM). Changes in the fluorescence intensity of Fluo-3 in 15 µm<sup>2</sup> of cytosol were analyzed at 515 nm by the laser confocal microscopy fitted with a × 40 oil objective. The results of Fluo-3 were expressed as the mean fluorescence intensity as arbitrary unit per cell. Intracellular fluorescence intensities of 25 cells were measured in the laser confocal microscope by ZEN program.

### Detection of Intracellular Reactive Oxygen Species (ROS) and Mitochondrial Membrane Potential Levels

Mitochondrial membrane depolarization and intracellular ROS production levels were assayed as described in previous studies [32, 33]. Briefly, cells were re-suspended in 0.2 ml of extracellular buffer and then incubated with DHR123 (1 µl) and JC1 (5 µl) dye solutions for 15 min at room temperature in dark. The samples were then analyzed by the laser confocal microscopy. JC1 (505 nm excitation, 535 emission) [35] and DHR123 (514 nm excitation, 570 emission) was excited with a diode laser at 488 nm, an Argon laser at 488 nm [34]. Fluorescence intensity in 15 µm<sup>2</sup> of each cell as arbitrary unit was measured by using ZEN program and analyzed using Image J/Imaris software. The results of JC1 and DHR123 were expressed as the mean fluorescence intensity as arbitrary unit/cell.

### Bride Field Images

Axiocam 702 mono is a high-performance sCMOS microscope camera with 2.3 megapixels and a sensor size of 1/1.2" (diagonal 13.3 mm). By the Zeiss company, the camera was adapted to the laser confocal microscope, and 3D bride field (BF) images.

### Caspase Assays

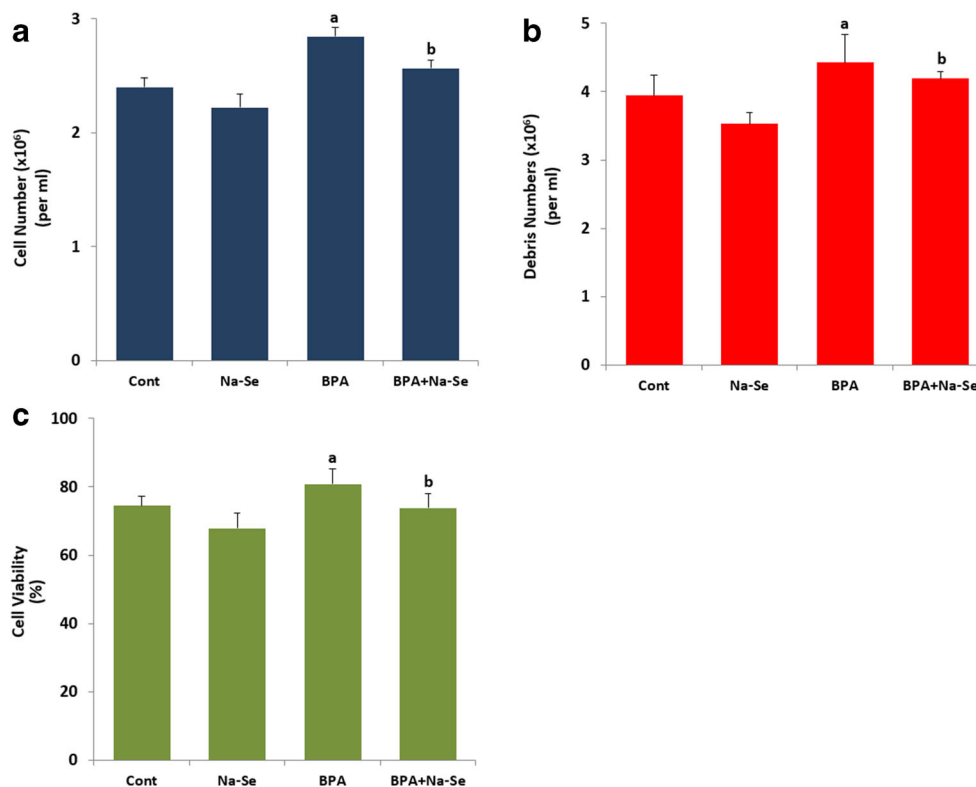
Caspase -3 and -9 activations are two reliable markers of apoptosis. Ac-DEVD-AMC and Ac-LEHD-AMC as two fluorogenic substrates can be used to continuously assay the activity of caspase -3 and -9 in cell extracts by using a spectrofluorometer or plate reader, respectively. The caspase -3 and -9 activities were

**Table 1** Effects of selenium (Na-Se) and bisphenol A (BPA) on reduced glutathione (rGSH), lipid peroxidation (LPx), and glutathione peroxidase (GSHPx) activity in the MCF-7 cells. (mean ± SD and *n* = 6)

Parameters	Control	Na-Se	BPA	BPA + Na-Se	BPA + Cpz
rGSH (µmol/g protein)	12.40 ± 0.45	13.10 ± 0.55	9.66 ± 0.30 <sup>a</sup>	9.80 ± 0.24 <sup>b</sup>	12.00 ± 0.51 <sup>b</sup>
GSHPx (IU/g protein)	19.73 ± 1.65	21.57 ± 1.72	13.58 ± 1.71 <sup>a</sup>	19.98 ± 1.33 <sup>b</sup>	17.15 ± 1.13 <sup>b</sup>
LPx (µmol/g protein)	20.40 ± 1.44	18.20 ± 0.20	23.20 ± 1.59 <sup>a</sup>	17.20 ± 0.70 <sup>b</sup>	18.80 ± 0.79 <sup>b</sup>

<sup>a</sup> *p* ≤ 0.05 versus control and Na-Se groups. <sup>b</sup> *p* ≤ 0.05 versus BPA group. (Kruskal-Wallis ANOVA test was used for the statistical analyses)

**Fig. 1** Effects of sodium selenite (Na-Se) on bisphenol A (BPA)-induced cell count (a), cell debris number (b), and cell viability level (c) in MCF-7 cells. (mean  $\pm$  SD and  $n = 3$ ). The cells were incubated with BPA (0.1 mM for 24 h) and then they were further incubated by Na-Se (1  $\mu$ M for 2 h). (<sup>a</sup> $p \leq 0.05$  versus control and Na-Se groups. <sup>b</sup> $p \leq 0.05$  versus BPA group. The data were analyzed by ANOVA)



assayed in a microplate reader (Infinite pro200; Tecan Austria GmbH, Groedig, Austria) by measuring the degradation of the Ac-DEVD-AMC and Ac-LEHD-AMC as previously described [36]. The data were calculated as fluorescence units/mg protein and presented as a % increase of control.

### Analyses of Reduced Glutathione (rGSH), Lipid Peroxidation (LPx) and Glutathione Peroxidase (GSHPx) Activity

rGSH and LPx levels in the MCF-7 cells were spectrophotometrically (Cary 60 UV-Vis Spectrophotometer, Agilent, İzmir, Turkey) analyzed at 412 nm and 532 nm by using the methods of Sedlak and Lindsay [37] and Placer et al. [38],

respectively. rGSH and LPx levels in the MCF-7 cells were indicated as  $\mu$ mol/g protein.

A spectrophotometric (Cary 60 UV) method was used in the cells for assaying GSHPx activity [39]. The activity of GSHPx is expressed as an international unit (IU) of GSH oxidized/min/g protein. The total protein in the supernatant of the cell homogenate was spectrophotometrically (Shimadzu UV-1800) assessed using the Bradford reagent at 595 nm.

### Statistical Analyses

All data were indicated as means  $\pm$  standard deviation (SD). To assess the differences between treatment groups for each treatment, we used the one-way ANOVA. We used a post hoc

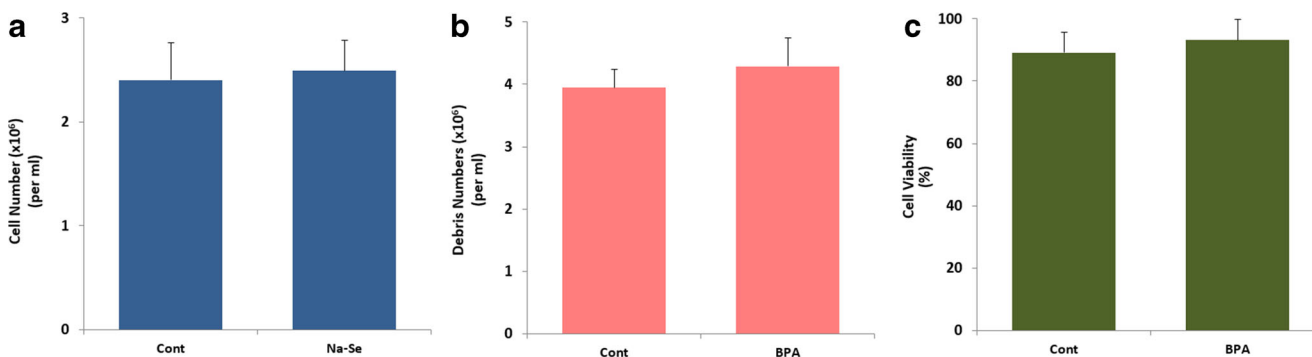


**Fig. 2** Effects of bisphenol A (BPA) on the cell count (a), cell debris number (b), and cell viability level (c) in the MDA-MB-231 cells. (mean  $\pm$  SD and  $n = 3$ ). The cells were incubated with BPA (0.1 mM for 24 h). Student's *t* test was used for the statistical analyses

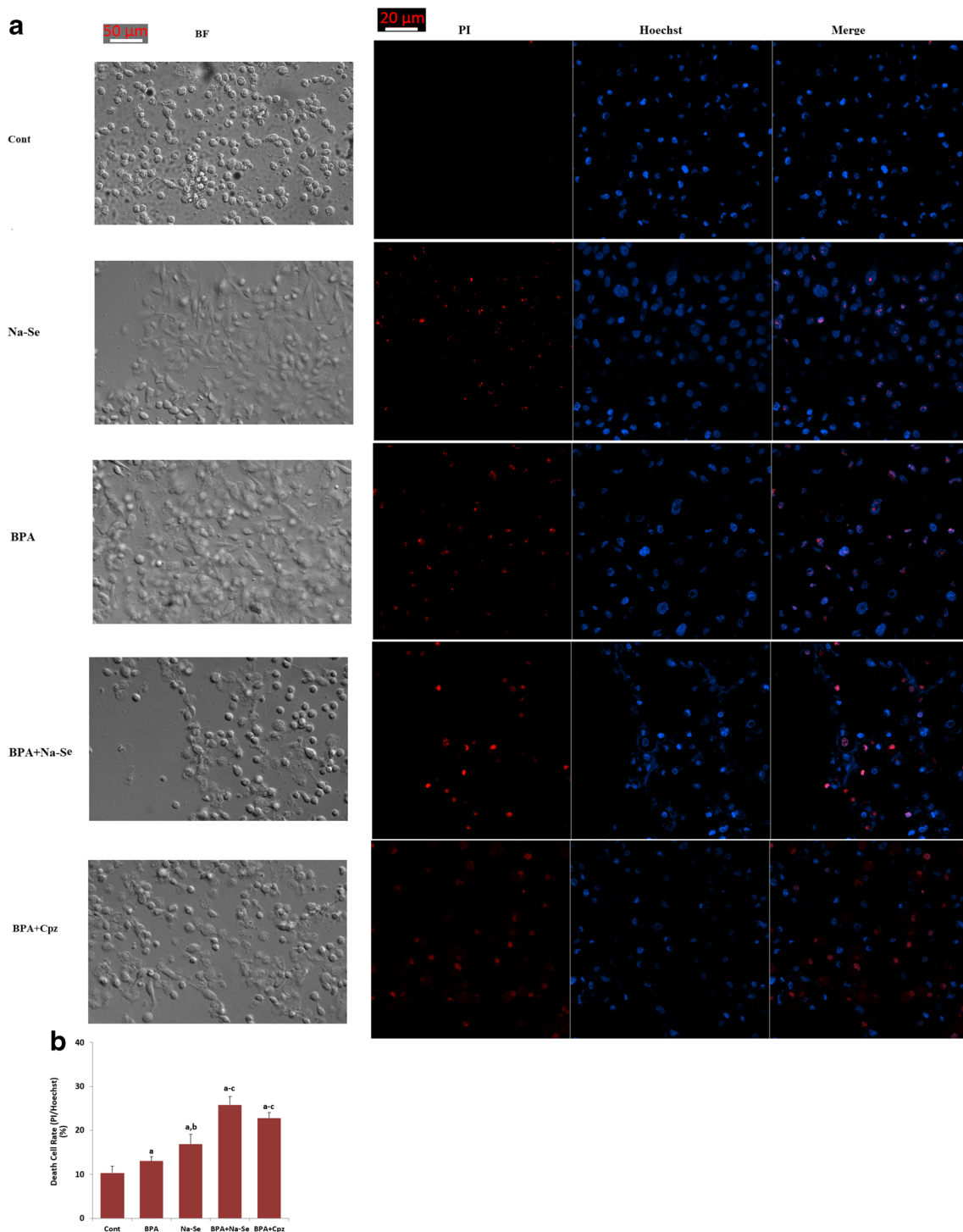


**Fig. 3** Sodium selenite (Na-Se) diminished bisphenol A (BPA)-induced cell death rate (PI/Hoechst) in the MCF-7 cells. The cells were stained with PI (5  $\mu\text{g}/\text{ml}$ ) and Hoechst 33342 (1  $\mu\text{M}$ ) (a and b) for detection of cell death and life cell ratio. Mean  $\pm$  SD of fluorescence per cell as arbitrary unit is presented. Summary of the mean values of PI and Hoechst cells under indicated conditions from  $n = 6$  independent

experiments, with each experiment examining 25 cells for each condition. The samples in the neuron death ( $\times 20$  objective) were analyzed by the laser confocal microscopy. (<sup>a</sup> $p \leq 0.05$  versus control and Na-Se groups. <sup>b</sup> $p \leq 0.05$  versus BPA group. The data were statistically significant by ANOVA)

test only when an ANOVA gave a statistically significant difference. When data did not pass the parametric test, we performed a Kruskal-Wallis ANOVA on ranks followed by a

Dunn's test (in Table 1 and Fig. 5). We used a Student  $t$  test when comparing two groups (in Figs. 2 and 4). Statistical probability of  $p \leq 0.05$  was considered significant.



## Results

### Na-Se Treatment Modulates BPA-Induced Changes of Cell Viability, Debris and Number in the MCF-7 255 but not in the MDA-MB-231 Cells

The cell number (Fig. 1a), debris amount (Fig. 1b), and cell viability (Fig. 1c) values in the MCF-7 cells were markedly higher in the BPA groups as compared to the control and Na-Se groups ( $p \leq 0.05$ ). However, the values were significantly ( $p \leq 0.05$ ) lower in the BPA + Na-Se group than in the BPA group. There was no difference in the cell number (Fig. 2a), debris amount (Fig. 2b), and cell viability (Fig. 2c) results of MDA-MB-231 cells between control and BPA groups.

### BPA-Induced Fluorescence Intensity of Cell Death (PI/Hoechst Rate) in the MCF-7 Cells but not in the MDA-MB-231 Cells Was Decreased by the Na-Se Treatment

Detections of cell death and cell viability in laser confocal microscopy analyses are more visible than in the cell counter

analyses. Hence, we imaged cell count as bride field (BF) and cell death in the laser confocal microscope analyses by using a camera and stain of death cells (PI) and stain of live cells (Hoechst). In the current study, the rate of cell death (Fig. 3a, b) in the MCF-7 cells of BPA group was higher than in the control and Na-Se groups ( $p \leq 0.05$ ). However, fluorescence intensities of the PI of Hoechst were diminished in the BPA + Na-Se groups of MCF-7 cells by the Na-Se treatment ( $p \leq 0.05$ ). However, there was no difference in the number of the death and live MDA-MB-231 cells between control and BPA groups (Fig. 4a, b). These imaging results further confirmed the protective role of Na-Se on the BPA-induced cell death in the MCF-7 cells.

### BPA-Induced Early and Late Apoptosis in the MCF-7 Cells Was Diminished by the Na-Se and Cpz Treatments

After observing a decrease of cell viability, but increase of cell death, we suspected increase of apoptosis in the MCF-7 cells. Hence, we imaged early (Annexin V-FITC) and late (PI) apoptosis levels in the laser confocal microscope analyses. In the current study, both Annexin V-FITC and PI levels were markedly ( $p \leq$

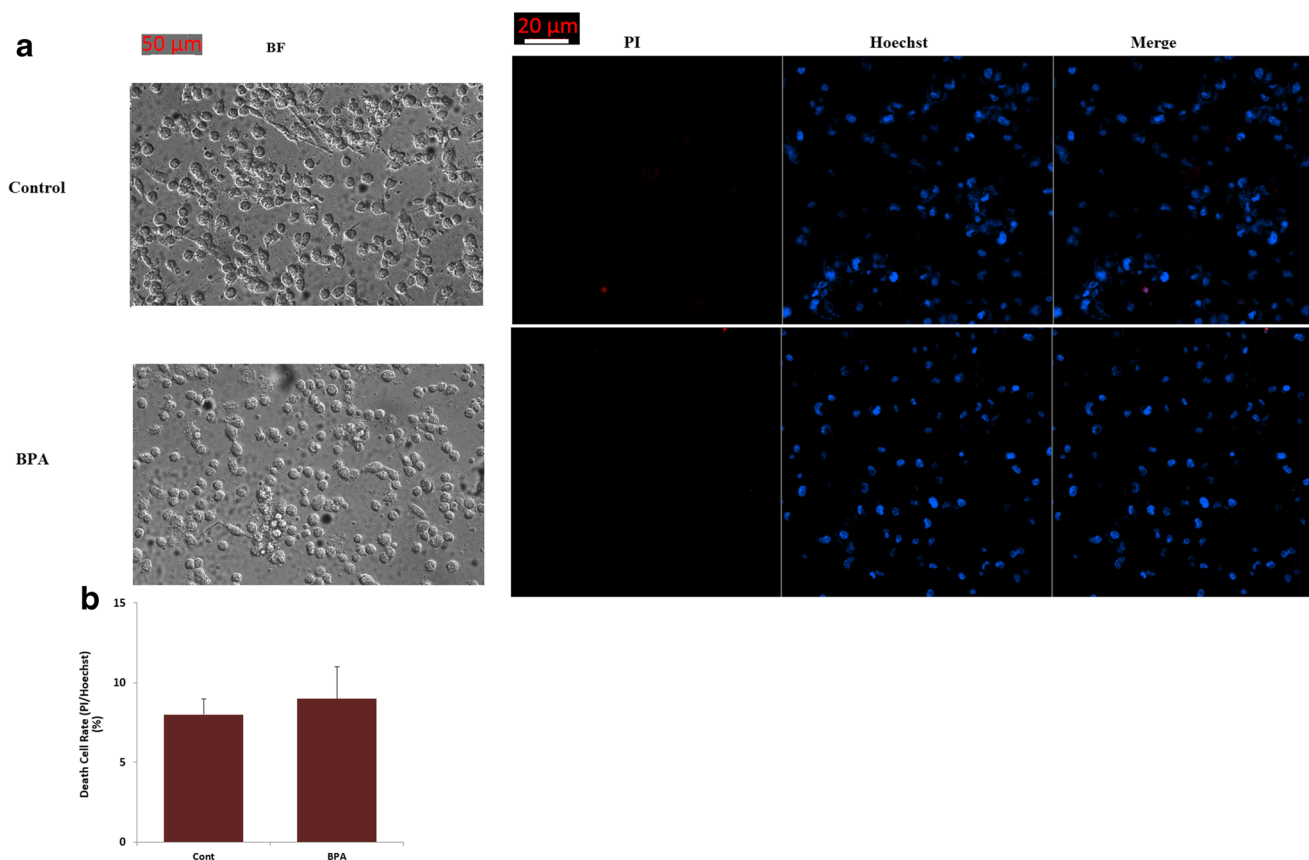


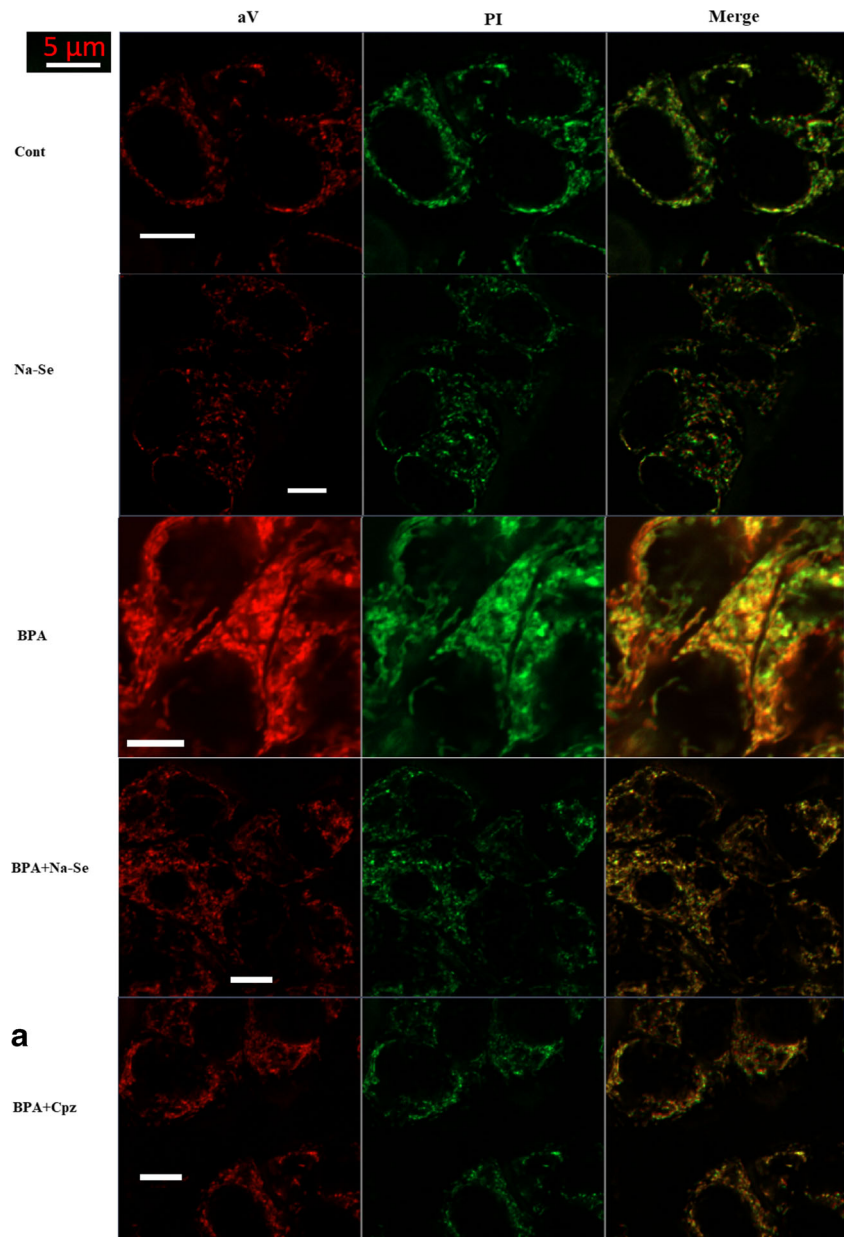
**Fig. 4** There is no effect of bisphenol A (BPA) on the cell death (PI/Hoechst) in the MDA-MB-231 cells. The cells were stained with PI (5 μg/ml) and Hoechst 33342 (1 μM) (a and b) for detection of cell death and life cell ratio. Mean ± SD of fluorescence per cell as arbitrary unit is presented. Summary of the mean values of PI and Hoechst cells under

indicated conditions from  $n = 6$  independent experiments, with each experiment examining 25 cells for each condition. The samples in the cancer cell death ( $\times 20$  objective) were analyzed by the laser confocal microscopy. Student's  $t$  test was used for the statistical analyses

0.05) increased in the BPA groups as compared to the control and Na-Se groups (Fig. 5a, b). However, fluorescence intensities of PI and Annexin V-FITC were decreased in the BPA + Na-Se

groups by the Na-Se and Cpz treatments ( $p \leq 0.05$ ). Fluorescence intensity of PI (late apoptosis) was markedly ( $p \leq 0.05$ ) higher than in the Annexin V-FITC (early apoptosis).

**Fig. 5** Effect of selenium (Na-Se, 1  $\mu$ M) and capsazepine (Cpz) on the levels of bisphenol A-induced caspase-3 and -9 activity in the MCF-7 (a) and MDA-MB-231 (b) cells. The cells in the caspase-3 and -9 assay were incubated with fluorogenic substrates (Ac-DEVD-AMC and Ac-LEHD-AMC). The samples were analyzed in the microplate reader (Infinite pro200). The cells were stimulated by Cap (10  $\mu$ M) and they were inhibited by Cpz (100  $\mu$ M). (<sup>a</sup> $p \leq 0.05$  versus control (Cont) and Na-Se groups. <sup>b</sup> $p \leq 0.05$  versus BPA group. \* $p \leq 0.05$  versus Cpz groups of Cont, Na-Se, BPA, and BPA + Na-Se). (Kruskal-Wallis test was used for the statistical analyses)



These imaging results further confirmed the protective roles of Na-Se and TRPV1 channel blocker (Cpz) on the BPA-induced apoptosis and cell death in the MCF-7 cells. In addition, it seems that cell death and apoptosis effects of BPA mostly occurred as late apoptosis instead of early apoptosis.

### BPA Increased Caspase -3 and -9 Activities in the MCF-7 Cells but not in the MDA-MB-231 Cells

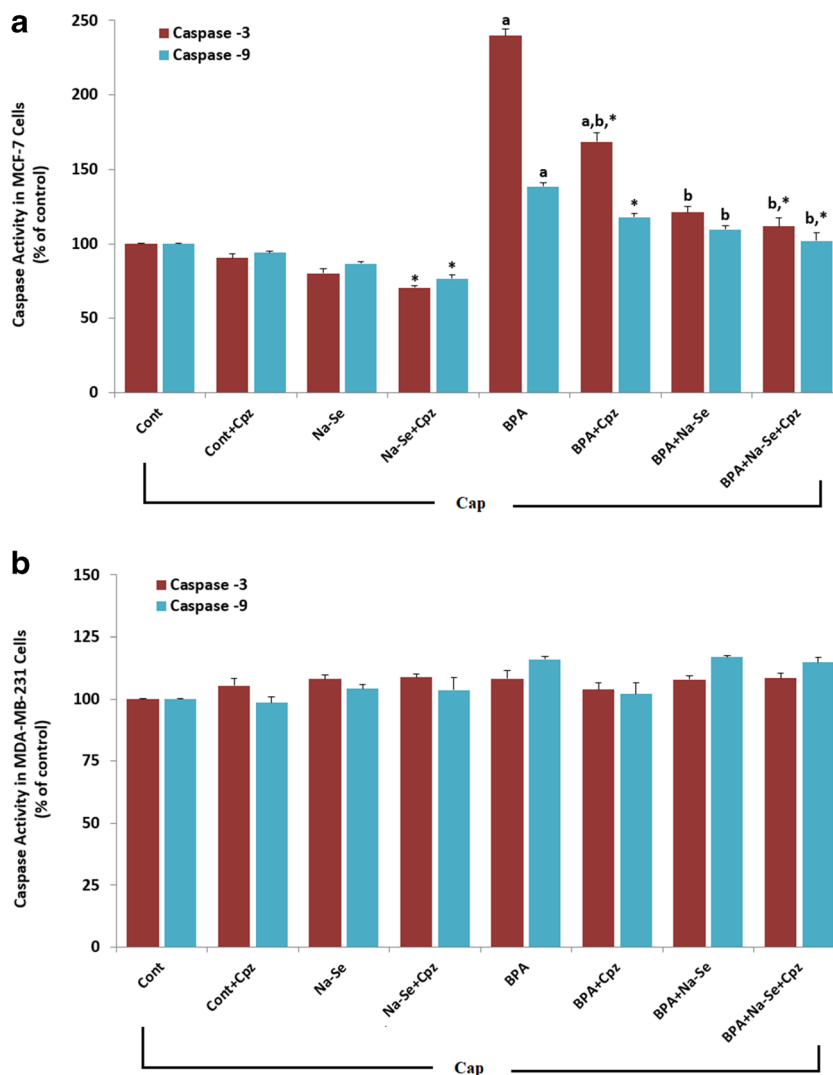
It is well known that the cell death, cell viability, and apoptosis values are induced in several cells by the increase of caspase -3 and -9 activities. After an observing increase of cell death and apoptosis in the MCF-7 cells but not in the MDA-MB-231 cells, we suspected increase of caspase -3 and -9 activities in the MCF-7 cells. Hence, we assayed the caspase activities in the MCF-7 cells. The results of caspase -3 and -9 activities in the four groups are shown in Fig. 6 through TRPV1 stimulation (Cap) and inhibition (Cpz). The caspase -3 and -9 activities in the MCF-7 cells were higher in the BPA groups

than in the control and Na-Se groups ( $p \leq 0.05$ ) (Fig. 6a). The caspase -3 and -9 activities in the MCF-7 cells were lower in the Na-Se groups than in the BPA group ( $p \leq 0.05$ ). In addition, the caspase -3 and -9 activities in the MCF-7 cells of four groups were further diminished by the Cpz treatments ( $p \leq 0.05$ ). However, there was no change in caspase -3 and -9 activities of MDA-MB-231 cells in the four groups (Fig. 6b). In addition, the caspase -3 and -9 activities of MDA-MB-231 cells were not affected by Cap and Cpz treatments.

### Na-Se Treatment Diminished BPA-Caused Increase of the $\text{Ca}^{2+}$ Fluorescence Intensity Through Inhibition of TRPV1 Activation

It is well known that an increase of intracellular  $\text{Ca}^{2+}$  concentration through activation of TRPV1 channel causes several physiological and pathophysiological functions including cancer cell proliferation [20, 21]. After observing an increase of cell numbers, we suspected increase of intracellular  $\text{Ca}^{2+}$

**Fig. 6** Sodium selenite (Na-Se) and capsazepine (Cpz) treatments diminished bisphenol A (BPA)-induced apoptosis level in MCF-7 cells. (mean  $\pm$  SD and  $n = 3$ ). a The cells were stained with PI (10  $\mu\text{g}/\text{ml}$ ) and aV (1  $\mu\text{M}$ ) (a and b) for detection of early (Annexin V, aV) and late (PI) apoptosis level. b Mean  $\pm$  SD of fluorescence per cell as arbitrary unit is presented. b Summary of the mean values of aV and PI cells under indicated conditions from  $n = 6$  independent experiments, with each experiment examining 25 cells for each condition. The samples in the cancer cell death ( $\times 40$  oil objective) were analyzed by the laser confocal microscopy. (<sup>a</sup> $p \leq 0.05$  versus control and Na-Se groups. <sup>b</sup> $p \leq 0.05$  versus BPA group. <sup>\*</sup> $p \leq 0.05$  versus PI group. The data were analyzed by ANOVA)





concentration in the MCF-7 cells. As the third step in the current study whether activation of TRPV1 is related to BPA treatment. The influences of the channel on intracellular  $\text{Ca}^{2+}$  accumulation were examined by measurement of  $\text{Ca}^{2+}$  concentration using the TRPV1 channel activator (Cap) and inhibitor (Cpz), respectively. The confocal microscope images (Fig. 7a) and columns (Fig. 7b) indicated that the  $\text{Ca}^{2+}$  concentration was increased in the BPA group by Cap stimulation (activation of TRPV1) and the  $\text{Ca}^{2+}$  fluorescence intensity was significantly ( $p \leq 0.05$ ) higher in the BPA group as compared to control and Na-Se groups. However, the  $\text{Ca}^{2+}$  concentration was decreased in the BPA + Na-Se group as compared to the BPA group ( $p \leq 0.05$ ). In addition, the fluorescence intensity of  $\text{Ca}^{2+}$  concentration was decreased by Cpz treatment and its concentration was markedly ( $p \leq 0.05$ ) lower in the Cpz groups (BPA + Cpz, Cont+Cpz, Na-Se + Cpz, and BPA + Na-Se + Cpz) than in the control and BPA group ( $p \leq 0.05$ ) (Fig. 7c). The Cpz results were obviously indicated involvement of BPA through activation of TRPV1 channel in the  $\text{Ca}^{2+}$  influx of MCF-7 cells.

### Na-Se Treatment Decreased BPA-Induced Mitochondrial Membrane Depolarization (JC-1) Level and Intracellular ROS (DHR123) Production

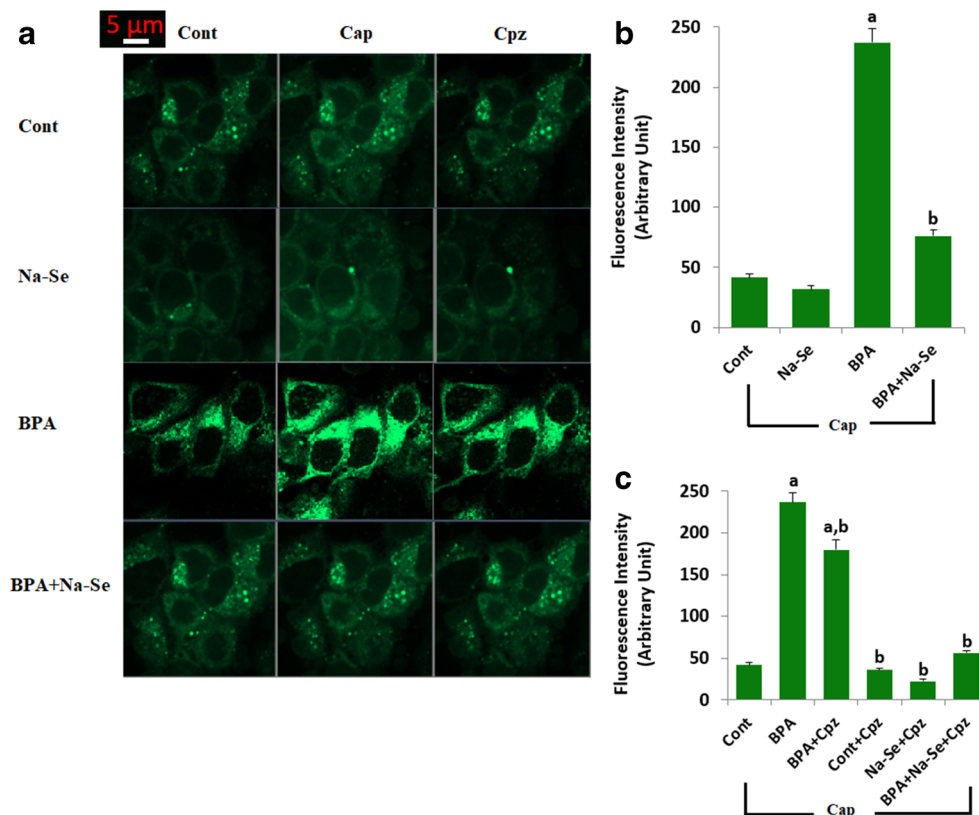
The level fluorescence intensity of laser confocal microscope images of JC-1 and DHR123 is shown in Fig. 8a, b. The fluorescence intensities of JC-1 and

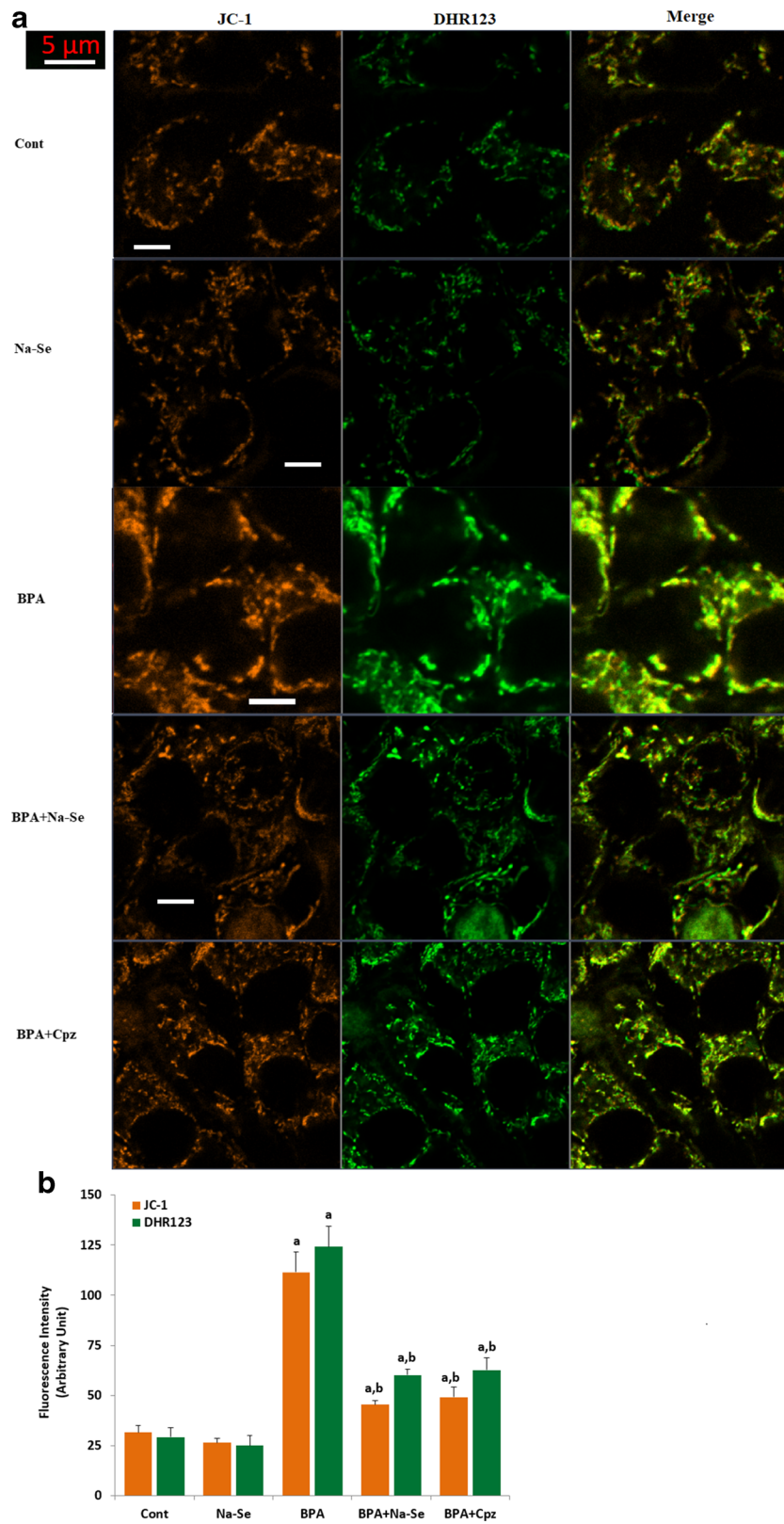
DHR were markedly ( $p \leq 0.05$ ) increased by BPA group. The JC-1 and DHR123 levels were markedly ( $p \leq 0.05$ ) lower in the BPA + Na-Se group as compared to BPA group. In addition, the JC-1 and DHR123 levels were markedly decreased by Cpz treatment and their levels were lower in the BPA + Cpz treatment groups than in the BPA group ( $p \leq 0.05$ ).

### Na-Se Treatment Decreased BPA-Induced Increase of LPx, Its Treatment Increased BPA-Induced Decrease of rGSH Level and GSHPx Activity in MCF-7 Cells

Results of LPx, rGSH, and GSHPx are shown in Table 1. The LPx level was markedly ( $p \leq 0.05$ ) higher in the BPA groups as compared to control and Na-Se groups, although its level was significantly ( $p \leq 0.05$ ) decreased in the BPA + Na-Se and BPA + Cpz groups by the Na-Se and Cpz treatments. However, the rGSH level and GSHPx activity were lower in the BPA group than in the control and Na-Se groups ( $p \leq 0.05$ ). However, the GSHPx activity and rGSH level were markedly ( $p \leq 0.05$ ) increased in the BPA + Na-Se and BPA + Cpz groups by the Na-Se and Cpz treatments. These findings clearly indicated that BPA-induced decrease of rGSH and GSHPx are increased by Na-Se treatment through downregulation of LPx and oxidative stress.

**Fig. 7** Effect of selenium (Na-Se, 1  $\mu\text{M}$ ) on the increase of bisphenol A (BPA)-induced  $\text{Ca}^{2+}$  fluorescence intensity through TRPV1 stimulation in the MCF-7 cells. (mean  $\pm$  SD and  $n = 6$ ). The cells were stained with  $\text{Ca}^{2+}$  indicator fluorescent dye and mean  $\pm$  SD of fluorescence in  $10 \text{ mm}^2$  of each cell as arbitrary unit are presented;  $n = 25$  independent experiments (a). The cells were activated by Cap (10  $\mu\text{M}$  for 10 min), but they were inhibited by Cpz (100  $\mu\text{M}$  for 10 min) after washing the Cap (a). The samples were analyzed by the laser confocal microscopy fitted with a  $\times 20$  objective. Changes of the  $\text{Ca}^{2+}$  fluorescence intensity after Cap (b) and Cpz (c) treatments were shown by columns. (<sup>a</sup> $p \leq 0.05$  versus control and Na-Se groups. <sup>b</sup> $p \leq 0.05$  versus BPA. The data were analyzed by ANOVA)





### Discussion

In the present study, we observed that BPA treatment activated the TRPV1 channel, resulting in the MCF-7 cancer

cell proliferation, overload  $Ca^{2+}$  entry, cell death, and mitochondria oxidative stress. More importantly, we found that the Na-Se could protect the MCF-7 cells from BPA-induced oxidative injury via maintaining the intracellular

**Fig. 8** Effect of selenium (Na-Se, 1  $\mu$ M) and capsazepine (Cpz) on the fluorescence intensity changes of bisphenol A-induced mitochondrial membrane depolarization (JC-1) (a) and intracellular ROS production (DHR123) (b) in the MCF-7 cells. The cells in the mitochondrial membrane depolarization and ROS analyses at room temperature in dark were stained with JC-1 and DHR123, respectively. Mean  $\pm$  SD of fluorescence per cell as arbitrary unit are presented;  $n = 25$  independent experiments. The samples were analyzed by the laser confocal microscopy fitted with a  $\times 20$  objective. (<sup>a</sup> $p \leq 0.05$  versus control and Na-Se groups. <sup>b</sup> $p \leq 0.05$  versus BPA. The data were analyzed by ANOVA)

$\text{Ca}^{2+}$  hemostasis and via stimulating late apoptosis pathways, as well as downregulating mitochondrial oxidative stress pathway. Na-Se induced TRPV1 modulator action through upregulation rGSH and GSHPx but downregulation of lipid peroxidation and mitochondria ROS production.

TRPV1 channel is activated in several cells, including MCF-7 by ROS and Cap [12, 13]. BPA induces excessive ROS production in the MCF-7 cell [40]. In addition, BPA induced estrogenic activity and  $\text{Ca}^{2+}$  influx in MCF-7 cells through activation of Erk and PI3K/Akt signals [41]. It was reported that BPA was further stimulated glutamate-induced  $\text{Ca}^{2+}$  influx through activation of NMDA receptors in rat hippocampus [42] and mouse pancreatic  $\beta$ -cells [43]. To our knowledge, there is no report interaction between the TRPV1 channel activity and MCF-7 oxidative toxicity. In the current study, we observed increased excessive mitochondria ROS production and  $\text{Ca}^{2+}$  influx through the TRPV1 channel activation in the MCF-7 cells. There are limited reports interactions between TRPV1 channel activator (Cap) and BPA and

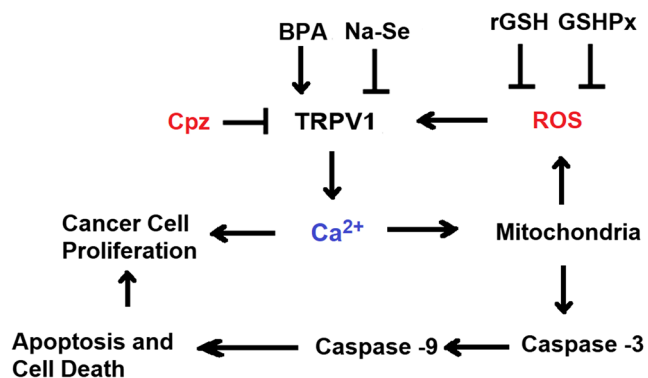


**Fig. 9** Molecular pathways on the inhibition of bisphenolA (BPA) caused the overload  $\text{Ca}^{2+}$  entry and cancer cell proliferation via TRPV1 channel activity modulation in the MCF-7 cells by sodium selenite (Na-Se) treatment. The overload  $\text{Ca}^{2+}$  entry causes increase of mitochondria membrane depolarization resulting in activation of two molecular pathways; (1) excessive ROS production in the mitochondria through decrease of reduced glutathione (rGSH) and glutathione peroxidase (GSHPx), (2) apoptosis through activation of caspase -3 and -9. However, Na-Se and TRPV1 antagonist (capsazepine, Cpz) protected the MCF-7 cells from BPA-induced injury downregulating mitochondrial oxidative stress and TRPV1 activity pathway

the reports are containing conflict results. It was reported that Cap-induced HT-29 human colon cancer death was completely blocked by BPA diglycidyl ether as a specific PPARgamma antagonist [44]. In rat testis cells, absence of relationship between Cap and BPA on  $\text{Ca}^{2+}$  influx was reported [45].

Na-Se is an inorganic form of selenium and it has antioxidant and  $\text{Ca}^{2+}$  channel modulator actions in several cells including MCF-7 [23, 25]. Oxidant effects of BPA were blocked in the lung [26], testis [27, 28], and liver of rats [29] by the Na-Se treatment. Antitumor and anti-apoptotic actions of Na-Se through upregulation of rGSH and GSHPx but downregulation of TRPV1 activity in MCF-7 cells [25], dorsal root ganglion neuron [30], and human osteoblast-like cell line [46] were recently reported. Increases of cancer cell proliferation, apoptosis, caspase -3 and -9 through activation of TRPV1 channel were also reported in the MCF-7 cells [15–18]. ROS are scavenged by rGSH and GSHPx. In the current study, GSHPx and rGSH values were downregulated in the MCF-7 cells by BPA, although their values were upregulated by the antioxidant property of Na-Se. After scavenging ROS by rGSH and GSHPx, the mitochondria membrane depolarization, ROS, and TRPV1 channel activity were diminished by the Na-Se and Cpz treatments.

It is well known that cancer cell proliferation needs excessive  $\text{Ca}^{2+}$  influx. It was also reported that there is a direct relationship between estrogen production and breast cancer tumor development [19]. In addition to the Cap and ROS, TRPV1 is also activated by estrogen [20, 21], although its activity was modulated in dorsal root ganglion and hippocampus of rats by estrogen receptor blockers [23]. In the current study, proliferation, cell death, and apoptosis values of estrogen receptor negative (MDA-MB-231) breast cancer cell were not affected by BPA and Na-Se treatments. However, estrogenic effect of BPA induced MCF-7 breast cancer cell proliferation and apoptosis via TRPV1 channel activation-induced  $\text{Ca}^{2+}$  influx, although the effects were modulated by the Na-Se treatment.

It is well known that increase of intracellular  $\text{Ca}^{2+}$  concentration stimulates breast cancer cell proliferation (Fig. 9). In addition, mitochondrial membrane depolarization in MCF-7 cells is induced by increase of intracellular  $\text{Ca}^{2+}$  concentration [47]. In turn, it results in activation of two molecular pathways; (1) excessive ROS production in the mitochondria is induced by the increase of  $\text{Ca}^{2+}$ -influx-caused mitochondrial membrane depolarization. (2) Apoptosis and cell death are activated through activation of caspase -3 and -9 [11] (Fig. 9). The TRPV1 activation-induced increase of mitochondria membrane depolarization, ROS production, apoptosis, caspase -3 and -9 activation were modulated in the MCF-7 cells by the Na-Se treatment [20]. In the current study, we observed



similar modulator action of Na-Se on the BPA-induced changes in the MCF-7 cells. The modulator action was attributed to the antioxidant and TRPV1 channel blocker actions of Na-Se.

In conclusion, BPA acted breast cancer proliferative effect in the estrogen receptor positive (MCF-7) breast cancer cells but not in the estrogen receptor negative (MDA-MB-231) breast cancer cell through stimulating  $\text{Ca}^{2+}$  entry (via TRPV1 activation) and mitochondria ROS production. The results provided a new molecular pathway for the study of breast cancer proliferation. However, Na-Se induced apoptotic, antioxidant, and anti-cell proliferative actions through modulation of the TRPV1 channel in the MCF-7 cells. Therefore, inhibition of TRPV1-mediated  $\text{Ca}^{2+}$  entry through Na-Se treatment may be a potential strategy for inhibiting BPA-induced proliferation the breast cancer cells.

**Authors' Contributions** DC and KGUG formulated the present hypothesis. MN was responsible for writing the report and analyzing the spectrophotometer, patch-clamp, and plate reader. DC and KGUG made also critical revision for the manuscript.

**Funding Information** The study was supported by the BSN Health, Analyses, Innovation, Consultancy, Organization, Agriculture and Industry LTD, Göller Bölgesi Teknokenti, Isparta, Turkey (Project No: 2018-22).

## Compliance with Ethical Standards

**Conflict of Interest** The authors declare that they have no conflict of interest.

**Ethical Approval** This article does not contain any studies with human and animal participants performed by any of the authors.

## References

- Gassman NR (2017) Induction of oxidative stress by bisphenol A and its pleiotropic effects. *Environ Mol Mutagen* 58:60–71
- Emfietzoglou R, Spyrou N, Mantzoros CS, Dalamaga M (2019) Could the endocrine disruptor bisphenol-A be implicated in the pathogenesis of oral and oropharyngeal cancer? Metabolic considerations and future directions. *Metabolism*. 91:61–69
- Shafei A, Ramzy MM, Hegazy AI, Husseny AK, el-Hadary UG, Taha MM, Mosa AA (2018) The molecular mechanisms of action of the endocrine disrupting chemical bisphenol A in the development of cancer. *Gene*. 647:235–243
- Galloway T, Cipelli R, Guralnik J, Ferrucci L, Bandinelli S, Corsi AM, Money C, McCormack P, Melzer D (2010) Melzer D. Daily bisphenol A excretion and associations with sex hormone concentrations: results from the InCHIANTI adult population study. *Environ Health Perspect* 118:1603–1608
- Wang Z, Liu H, Liu S (2016) Low-dose bisphenol A exposure: a seemingly instigating carcinogenic effect on breast cancer. *Adv Sci (Weinh)* 4(2):1600248
- Leung YK, Govindarajah V, Cheong A, Veevers J, Song D, Gear R, Zhu X, Ying J, Kandler A, Medvedovic M, Belcher S, Ho SM (2017) Gestational high-fat diet and bisphenol A exposure heightens mammary cancer risk. *Endocr Relat Cancer* 24(7):365–378
- Nazıroğlu M (2007) New molecular mechanisms on the activation of TRPM2 channels by oxidative stress and ADP-ribose. *Neurochem Res* 32:1990–2001
- Bong AHL, Bassett JJ, Roberts-Thomson SJ, Monteith GR (2019) Assessment of doxorubicin-induced remodeling of  $\text{Ca}^{2+}$  signaling and associated  $\text{Ca}^{2+}$  regulating proteins in MDA-MB-231 breast cancer cells. *Biochem Biophys Res Commun* 522(2):532–538
- Nazıroğlu M, Yüksel M, Köse SA, Özkaya MO (2013) Recent reports of Wi-Fi and mobile phone-induced radiation on oxidative stress and reproductive signaling pathways in females and males. *J Membr Biol* 246:869–875
- Nazıroğlu M, Blum W, Jósavay K, Çiğ B, Henzi T, Oláh Z, Vizler C, Schwaller B, Pecze L (2018) Menthol evokes  $\text{Ca}^{2+}$  signals and induces oxidative stress independently of the presence of TRPM8 (menthol) receptor in cancer cells. *Redox Biol* 14:439–449
- Carrasco C, Nazıroğlu M, Rodríguez AB, Pariente JA (2018) Neuropathic pain: delving into the oxidative origin and the possible implication of transient receptor potential channels. *Front Physiol* 9: 95
- Caterina MJ, Schumacher MA, Tominaga M, Rosen TA, Levine JD, Julius D (1997) The capsaicin receptor: a heat-activated ion channel in the pain pathway. *Nature* 389:816–824
- Susankova K, Tousova K, Vyklicky L, Teisinger J, Vlachova V (2006) Reducing and oxidizing agents sensitize heat-activated vanilloid receptor (TRPV1) current. *Mol Pharmacol* 70:83–394
- Vercelli C, Barbero R, Cuniberti B, Odore R, Re G (2015) Expression and functionality of TRPV1 receptor in human MCF-7 and canine CF.41 cells. *Vet Comp Oncol* 13:133–142
- Wu TT, Peters AA, Tan PT, Roberts-Thomson SJ, Monteith GR (2014) Consequences of activating the calcium-permeable ion channel TRPV1 in breast cancer cells with regulated TRPV1 expression. *Cell Calcium* 56(2):59–67
- Çiğ B, Nazıroğlu M (2015) Investigation of the effects of distance from sources on apoptosis, oxidative stress and cytosolic calcium accumulation via TRPV1 channels induced by mobile phones and Wi-Fi in breast cancer cells. *Biochim Biophys Acta* 1848(10 Pt B): 2756–2765
- Nur G, Nazıroğlu M, Deveci HA (2017) Synergic prooxidant, apoptotic and TRPV1 channel activator effects of alpha-lipoic acid and cisplatin in MCF-7 breast cancer cells. *J Recept Signal Transduct Res* 37:569–577
- Deveci HA, Nazıroğlu M, Nur G (2018) 5-Fluorouracil-induced mitochondrial oxidative cytotoxicity and apoptosis are increased in MCF-7 human breast cancer cells by TRPV1 channel activation but not Hypericum perforatum treatment. *Mol Cell Biochem* 439(1–2):189–198
- Rausch LK, Netzer NC, Hoegel J, Pramsöhler S (2017) The linkage between breast cancer, hypoxia, and adipose tissue. *Front Oncol* 7: 211
- Lozano C, Córdova C, Marchant I et al (2018) Intracellular aggregated TRPV1 is associated with lower survival in breast cancer patients. *Breast Cancer (Dove Med Press)* 10:161–168
- Gonçalves R, Zanatta AP, Cavalari FC, do Nascimento MAW, Delalande-Lecapitaine C, Bouraïma-Lelong H, Silva FRMB (2018) Acute effect of bisphenol A: signaling pathways on calcium influx in immature rat testes. *Reprod Toxicol* 77:94–102
- Yazgan Y, Nazıroğlu M (2017) Ovariectomy-induced mitochondrial oxidative stress, apoptosis, and calcium ion influx through TRPA1, TRPM2, and TRPV1 are prevented by 17 $\beta$ -estradiol, tamoxifen, and raloxifene in the hippocampus and dorsal root ganglion of rats. *Mol Neurobiol* 54(10):7620–7638
- Wagner MS, Schultze E, Oliveira TL et al (2018) Revitalizing the AZT through of the selenium: an approach in human triple negative breast cancer cell line. *Front Oncol* 8:525

24. Abd-Rabou AA, Shalby AB, Ahmed HH (2019) Selenium nanoparticles induce the chemo-sensitivity of fluorouracil nanoparticles in breast and colon cancer cells. *Biol Trace Elem Res* 187(1):80–91
25. Sakallı Çetin E, Nazıroğlu M, Çiğ B, Övey İS, Aslan KP (2017) Selenium potentiates the anticancer effect of cisplatin against oxidative stress and calcium ion signaling-induced intracellular toxicity in MCF-7 breast cancer cells: involvement of the TRPV1 channel. *J Recept Signal Transduct Res* 37:84–93
26. Abedelhaffez AS, El-Aziz EAA, Aziz MAA, Ahmed AM (2017) Lung injury induced by Bisphenol A: a food contaminant, is ameliorated by selenium supplementation. *Pathophysiology* 24(2):81–89
27. Kaur S, Saluja M, Bansal MP (2018) Bisphenol A induced oxidative stress and apoptosis in mice testes: modulation by selenium. *Andrologia* 50(3):e12834
28. Khalaf AA, Ahmed W, Moselhy WA, Abdel-Halim BR, Ibrahim MA (2019 Apr) Protective effects of selenium and nano-selenium on bisphenol-induced reproductive toxicity in male rats. *Hum Exp Toxicol* 38(4):398–408
29. Amraoui W, Adjabi N, Bououza F et al (2018) Modulatory role of selenium and vitamin E, natural antioxidants, against Bisphenol A-induced oxidative stress in Wistar Albinos ats. *Toxicol Res* 34(3): 231–239
30. Yüksel E, Nazıroğlu M, Şahin M, Çiğ B (2017) Involvement of TRPM2 and TRPV1 channels on hyperalgesia, apoptosis and oxidative stress in rat fibromyalgia model: protective role of selenium. *Sci Rep* 7(1):17543
31. Kim JY, Choi HG, Lee HM, Lee GA, Hwang KA, Choi KC (2017) Effects of bisphenol compounds on the growth and epithelial mesenchymal transition of MCF-7 CV human breast cancer cells. *J Biomed Res* 31(4):358–369
32. Ertilav K, Nazıroğlu M, Ataizi ZS, Braidy N (2019) Selenium enhances the apoptotic efficacy of docetaxel through activation of TRPM2 channel in DBTRG glioblastoma cells. *Neurotox Res* 35(4):797–808
33. Gökçe Kütük S, Gökçe G, Kütük M, Gürses Cila HE, Nazıroğlu M (2019) Curcumin enhances cisplatin-induced human laryngeal squamous cancer cell death through activation of TRPM2 channel and mitochondrial oxidative stress. *Sci Rep* 9(1):17784
34. Pariente R, Pariente JA, Rodríguez AB, Espino J (2016) Melatonin sensitizes human cervical cancer HeLa cells to cisplatin-induced cytotoxicity and apoptosis: effects on oxidative stress and DNA fragmentation. *J Pineal Res* 60(1):55–64
35. Joshi DC, Bakowska JC (2011) Determination of mitochondrial membrane potential and reactive oxygen species in live rat cortical neurons. *J Vis Exp* 51:2704
36. Oz A, Celik O, Ovey IS (2017) Effects of different doses of curcumin on apoptosis, mitochondrial oxidative stress and calcium influx in DBTRG glioblastoma cells. *J Cell Neurosci Oxid Stress* 9: 617–629
37. Sedlak J, Lindsay RHC (1966) Estimation of total, protein bound and non-protein sulfhydryl groups in tissue with Ellmann's reagent. *Anal Biochem* 25:192–205
38. Placer ZA, Cushman L, Johnson BC (1966) Estimation of products of lipid peroxidation (malonyl dialdehyde) in biological fluids. *Anal Biochem* 16:359–364
39. Lawrence RA, Burk RF (1976) Glutathione peroxidase activity in selenium-deficient rat liver. *Biochem Biophys Res Commun* 71: 952–958
40. Lei B, Sun S, Xu J, Feng C, Yu Y, Xu G, Wu M, Peng W (2018) Low-concentration BPAF- and BPF-induced cell biological effects are mediated by ROS in MCF-7 breast cancer cells. *Environ Sci Pollut Res Int* 25(4):3200–3208
41. Lei B, Sun S, Zhang X, Feng C, Xu J, Wen Y, Huang Y, Wu M, Yu Y (2019) Bisphenol AF exerts estrogenic activity in MCF-7 cells through activation of Erk and PI3K/Akt signals via GPER signaling pathway. *Chemosphere* 220:362–370
42. Zhong X, Li J, Zhuang Z, Shen Q, Jiang K, Hu Y, Wu D, Xu X (2019) Rapid effect of bisphenol a on glutamate-induced Ca(2+) influx in hippocampal neurons of rats. *Mol Cell Endocrinol* 485: 35–43
43. Villar-Pazos S, Martinez-Pinna J, Castellano-Muñoz M, Alonso-Magdalena P, Marroqui L, Quesada I, Gustafsson JA, Nadal A (2017) Molecular mechanisms involved in the non-monotonic effect of bisphenol-a on Ca<sup>2+</sup> entry in mouse pancreatic  $\beta$ -cells. *Sci Rep* 7(1):11770
44. Kim CS, Park WH, Park JY, Kang JH, Kim MO, Kawada T, Yoo H, Han IS, Yu R (2004) Capsaicin, a spicy component of hot pepper, induces apoptosis by activation of the peroxisome proliferator-activated receptor gamma in HT-29 human colon cancer cells. *J Med Food* 7(3):267–273
45. Gonçalves R, Zanatta AP, Cavalari FC, do Nascimento MAW, Delalande-Lecapitaine C, Bouraïma-Lelong H, Silva FRMB (2018) Acute effect of bisphenol A: signaling pathways on calcium influx in immature rat testes. *Reprod Toxicol* 77:94–102
46. Yazıcı T, Koçer G, Nazıroğlu M, Övey İS, Öz A (2018) Zoledronic acid, bevacizumab and dexamethasone-induced apoptosis, mitochondrial oxidative stress, and calcium signaling are decreased in human osteoblast-like cell line by selenium treatment. *Biol Trace Elem Res* 184(2):358–368
47. Lakshmi Priya T, Soumya T, Jayasree PR, Manish Kumar PR (2018) Selective induction of DNA damage, G2 abrogation, and mitochondrial apoptosis by leaf extract of traditional medicinal plant *Wrightia arborea* in K562 cells. *Protoplasma*. 255(1):203–216

**Publisher's Note** Springer Nature remains neutral with regard to jurisdictional claims in published maps and institutional affiliations.